

## A Pedal Dynamometer for Off-Road Bicycling

T. Rowe,<sup>1,4</sup> M. L. Hull,<sup>2,4</sup> and E. L. Wang<sup>3,5</sup>

*This paper describes the design and accuracy evaluation of a dynamometric pedal, which measures the two pedal force components in the plane of the bicycle. To realize a design that could be used during actual off-road cycling, a popular clipless pedal available commercially was modified so that both the form and the function of the original design were maintained. To measure the load components of interest, the pedal spindle was replaced with a spindle fixed to the pedal body and instrumented with eight strain gages connected into two Wheatstone bridge circuits. The new spindle is supported by bearings in the crank arm. Static calibration and a subsequent accuracy check revealed root mean square errors of less than 1 percent full scale (FS) when only the force components of interest were applied. Application of unmeasured load components created an error less than 2 percent FS. The natural frequency with half the weight of a 75 kgf person standing on the pedal was greater than 135 Hz. These performance capabilities make the dynamometer suitable for measuring either pedaling loads due to the rider's muscular action or inertial loads due to surface-induced acceleration. To demonstrate this suitability, sample pedal load data are presented both for steady-state ergometer cycling and coasting over a rough surface while standing.*

### Introduction

Quantifying the pedal loads is an important step toward understanding the relationship between the rider and the bicycle during off-road riding. Better understanding of this relationship lets bicycle designers design more efficient and ergonomic bicycles. Also, the pedal loads give insight into the biomechanics of bicycling and the injuries associated with pedaling. Finally, the stresses in bicycle components may be derived from the pedal loads, allowing structural optimization.

<sup>1</sup> Research Assistant.

<sup>2</sup> Professor.

<sup>3</sup> Assistant Professor.

<sup>4</sup> Department of Mechanical Engineering, University of California, Davis, Davis, CA 95616.

<sup>5</sup> Department of Mechanical Engineering, University of Nevada, Reno, NV 89557.

Contributed by the Bioengineering Division of THE AMERICAN SOCIETY OF MECHANICAL ENGINEERS. Manuscript received by the Bioengineering Division May 23, 1996; revised manuscript received December 21, 1996. Associate Technical Editor: A. G. Erdman.

In designing a dynamometric pedal for off-road use, it is useful to consider the design criteria. To operate reliably in the off-road environment, a dynamometric pedal needs to be structurally equivalent to current clipless pedals. Structural equivalence means that the dynamometric pedal must withstand the loading developed not only as a consequence of foot-pedal interaction, but also as a consequence of pedal-ground interaction. Thus, the pedal must be sturdy enough to avoid failure upon contact with obstacles as well as support high-magnitude inertial loads that develop while traveling over a rough surface (Wilczynski and Hull, 1994).

In addition to structural equivalence, the design must also be functionally equivalent to current pedals. Functional equivalence is important to gaining a realistic picture of the loading. To achieve functional equivalence, the physical dimensions must be comparable to limit contact with obstacles. Additionally, the pedal must be of a clipless design to accommodate common mountain biking shoes. Finally, the instrumentation must be protected from dirt and water to allow operation in the harsh off-road environment.

Another consideration is that the dynamometer must accurately measure the two in-plane force components (Fig. 1) because these are of primary interest in off-road bicycling.  $F_x$  and  $F_z$  (the tangential and normal pedal forces) are the two primary driving forces and are the greatest in magnitude of the six loads typically applied while pedaling (Hull and Davis, 1981). Additionally, it is anticipated that the surface-induced inertial loads will be greatest primarily in the plane of the bicycle. The results of a dynamic simulation support this assumption (Wilczynski and Hull, 1994). To gain high accuracy, the cross sensitivity to the four unmeasured load components should be negligible since these are not measured.

A number of pedal dynamometers capable of measuring the in-plane loads have been described in the literature, but none satisfy the criteria for an off-road application. The two force component dynamometers developed by Soden and Adeyefa (1979) and Newmiller et al. (1988) gained insensitivity to extraneous loads through mechanical decoupling. Although these designs accurately indicate the two force components of interest, both are too large for off-road use. Recently, a compact two-force component dynamometer was constructed for road use (Viñolas and Alvarez, 1992). An off-road dynamometer design needs to be more durable than a road design, however. Off-road shoes also need to be accommodated in the design. Because none of the designs described above was suitable for the off-road application, the objective of this work was to design, construct, and evaluate a two-load component pedal dynamometer for off-road use.

### Methods and Materials

The pedal dynamometer was fabricated by modifying a Shimano SPD 737 clipless pedal. The primary modification consisted of relocating the bearings from their normal housing in

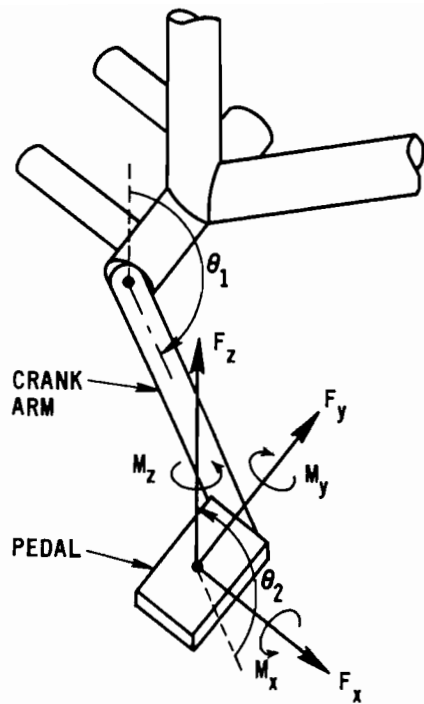


Fig. 1 Pedal coordinate system: The dynamometer measured the normal  $F_z$  and tangential  $F_x$  force components. Both the relative angle ( $\theta_2$ ) between the pedal and crank arm and the angle between the crank arm and frame ( $\theta_1$ ) were measured by potentiometers.

the pedal body to a housing in the crank arm so that the spindle would not rotate relative to the pedal (Fig. 2). Because of the large moment developed by the pedal forces at the crank due to the lever arm of the pedal, a two-bearing design was used. A ball bearing absorbs the thrust load ( $F_y$ ) while a cylindrical roller bearing supports the large moment. The bearing size was chosen based on the conflicting requirements of load capacity and mounting space available in the crank arm. The dynamic

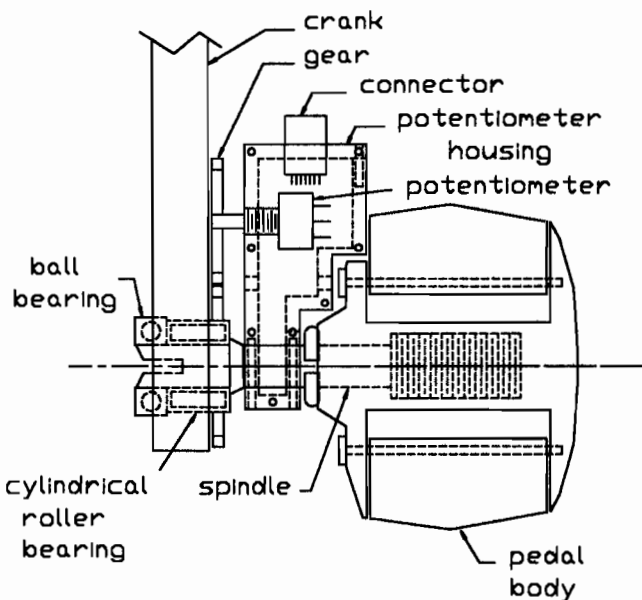


Fig. 2 Assembly showing modifications to the commercially available pedal: The pedal body was retained but the spindle and bearings originally within the body were removed. The spindle was replaced with a special design to meet sensitivity and strength requirements and the bearings were relocated to the crank arm.

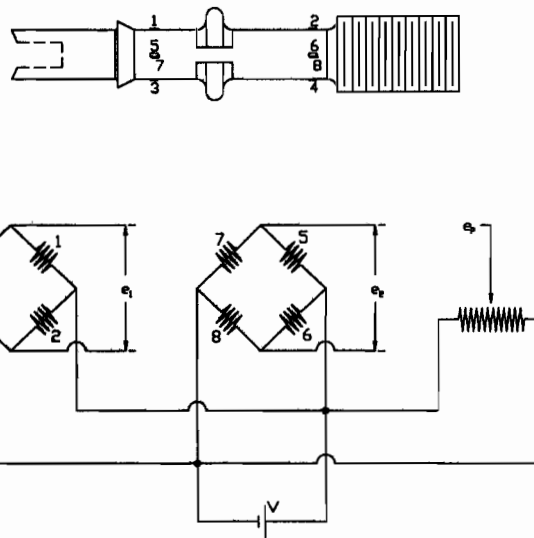


Fig. 3 Strain gage placement and wiring:  $V$  is the excitation voltage,  $e_1$  and  $e_2$  are the bridge outputs, and  $e_p$  is the potentiometer output

load rating for the bearings used is 3700 N and 5930 N for the ball and cylindrical roller bearing, respectively. The maximum load anticipated is 8000 N. This load would be produced when an 890 N load is applied to the pedal.

To provide signals indicating the two loads, the pedal spindle was instrumented with eight strain gages fixed at 90 deg intervals about the longitudinal axis at two locations (Fig. 3). Four strain gages in each of two perpendicular planes were interconnected into two complete Wheatstone bridges (corresponding to the  $F_x$  and  $F_z$  output signals). The location and interconnection of the gages not only renders the dynamometer insensitive to the location of forces  $F_x$  and  $F_z$  but also eliminates in theory cross sensitivity to all three moments and the third force component  $F_y$ .

The pedal spindle geometry was governed by the bearing size and the desired strain for the gages. The spindle has the smallest factor of safety at the bearing sites with a diameter of 9.52 mm. These dimensions were necessary due to the crank arm size limiting the bearing size. The same spindle diameter at the strain gage locations was determined to produce 2000 microstrain under an 890 N load. Since 9.52 mm is significantly smaller than the 12.45 mm of the 4130-Cromoly SPD 737 pedal spindle, the pedal spindle was made from 17-4 PH stainless steel, which has a yield strength ( $S_y = 1175$  MPa) more than twice that of Cromoly ( $S_y = 550$  MPa) in an untreated form.

A potentiometer was used to measure the angle of the pedal relative to the crank arm ( $\theta_2$  in Fig. 1). The potentiometer was located behind the spindle and was protected by a small aluminum box, which also protects the wiring and strain gages from impact damage and contamination (Figs. 2 and 4). Because a gear train with a one-to-one ratio drives the remotely located potentiometer, the potentiometer directly indicates the angle of the pedal with respect to the crank.

Another potentiometer monitors the crank angle with respect to the bicycle frame ( $\theta_1$  in Fig. 1). When used in conjunction with the pedal angle potentiometer, the angle between the pedal and bicycle frame may be computed.

### Calibration

Static calibration of the instrumented pedal was performed on the same apparatus as that described by Hull and Davis (1981). This apparatus is capable of applying the three forces and three moments to a bicycle pedal using a system of weights and pulleys. For all load components except the  $M_y$

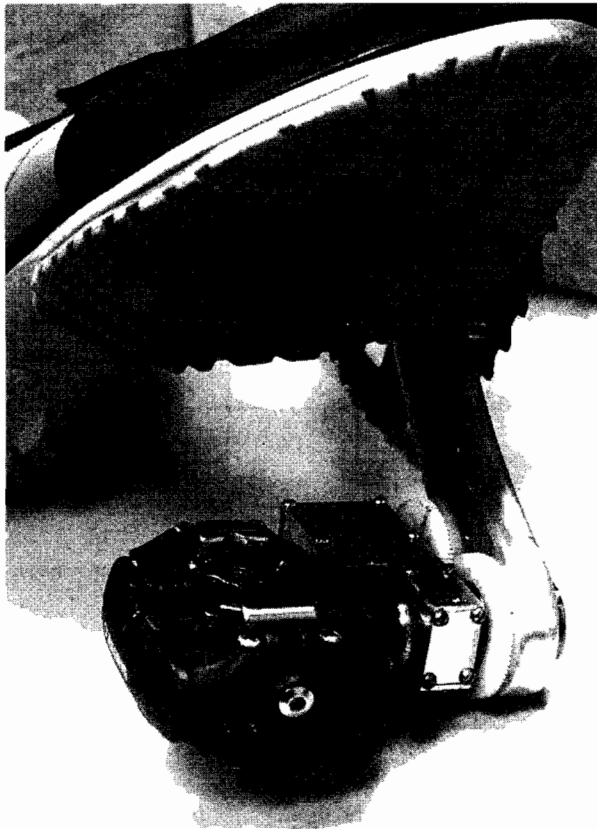


Fig. 4 Photograph of dynamometer: The dynamometer appears identical to a commercially available design except for the housing and gears, which protect and drive the potentiometer, respectively.

moment, weights were added up to the maximum and then subtracted in both polarity directions to give a complete cycle of loading. The  $M_y$  moment was not applied because this moment is produced from bearing friction and thus can be neglected. The maximum force applied in the  $x$  and  $z$  directions was 942 N. For the  $y$  direction a force of 312 N was applied. The  $x$  and  $z$  moments each received a maximum of 18 Nm.

The direct sensitivity and both the calibratable and non-calibratable cross sensitivities of the pedal were found with the data collected from the calibration procedure. Direct sensitivity is the response of a strain gage circuit to a load that the circuit is designed to measure (i.e., circuit 1 responding to  $F_x$ ). Calibratable cross sensitivity is the response of a circuit to the other load components being measured (i.e., circuit 2 responding to  $F_x$ ). Non-calibratable cross sensitivity is the response generated by a load that the circuit is not designed to measure (i.e., circuit 1 and/or circuit 2 responding to  $M_x$ ,  $M_z$ , or  $F_y$ ). Linear regression on the output voltage versus loading data was used to determine the slopes that indicate the various sensitivities.

Although the sensitivity matrix revealed some calibratable cross sensitivity between  $F_x$  and  $F_z$  (Table 1), the cross-sensitive coefficients were more than 20 times less than the direct-sensitive coefficients, which were equal. Both the direct and cross sensitivities were extremely linear (minimum R-square

Table 1 Calibratable sensitivity matrix [Volts/Newton] (normalized for gain and input voltage)

$$\begin{bmatrix} V_x \\ V_z \end{bmatrix} = \begin{bmatrix} +1.94E - 6 & -7.67E - 8 \\ +9.73E - 8 & +1.94E - 6 \end{bmatrix} \begin{bmatrix} F_x \\ F_z \end{bmatrix}$$

Table 2 Non-calibratable sensitivity matrix [Volts/Newton or Volts/Newton-meter] (normalized for gain and input voltage)

$$\begin{bmatrix} V_x \\ V_z \end{bmatrix} = \begin{bmatrix} +1.26E - 8 & -5.67E - 7 & +2.09E - 7 \\ -3.14E - 9 & -4.84E - 7 & -1.89E - 6 \end{bmatrix} \begin{bmatrix} F_y \\ M_x \\ M_z \end{bmatrix}$$

value of 0.995). Because of the linearity, the cross sensitivity may be accounted for in the calibration matrix (i.e., inverse of sensitivity matrix) to minimize the error.

The non-calibratable cross sensitivity of the dynamometer to the  $F_y$  force was found to be minimal (Table 2), but the non-calibratable cross sensitivities to the  $M_x$  and  $M_z$  moments were large. Because the strains in all four gages must be equal in magnitude if the cross sensitivity to bending is to be eliminated, the large cross sensitivity to  $M_x$  and  $M_z$  moments was likely due to gage misalignments. The worst case was for  $V_z$  in response to  $M_z$  where the cross sensitivity was nearly equal to the direct sensitivities in Table 1. The large cross sensitivities to moment load components will not lead to large errors, however, because the maximum moment loads are relatively small. Using experimental maximum moment loads of 18 Nm (Stone, 1990), the largest response was 0.6 and 1.8 percent of the full scale (FS) reading (890 N) for the  $x$  and  $z$  directions, respectively. The  $F_y$  force applied was 312 N and resulted in a maximum error of 0.4 percent FS.

An accuracy check of the dynamometer was performed after the calibration process using 16 combinations of the in-plane force components. These combinations spanned the entire expected load range of  $F_x$  and  $F_z$ . The output voltage of the bridges was recorded, and the forces were calculated using the calibration matrix previously discussed. The largest errors corresponded to 1.9 and 0.7 percent FS for the  $x$  and  $z$  directions, respectively, and were only found in cases of extreme loading. The root mean squared errors (RMSE's) were found to be 0.8 percent FS and 0.4 percent FS for the  $x$  and  $z$  directions, respectively.

The hysteresis of the dynamometer was also determined from the calibration data. Since the loading sequences were cyclic, the hysteresis error was computed for both positive and negative loading directions in the calibration cycles. The hysteresis introduced a maximum error of less than 1.1 percent FS.

In addition to the static calibration, the natural frequency of the pedal was determined along the  $z$  axis to characterize the

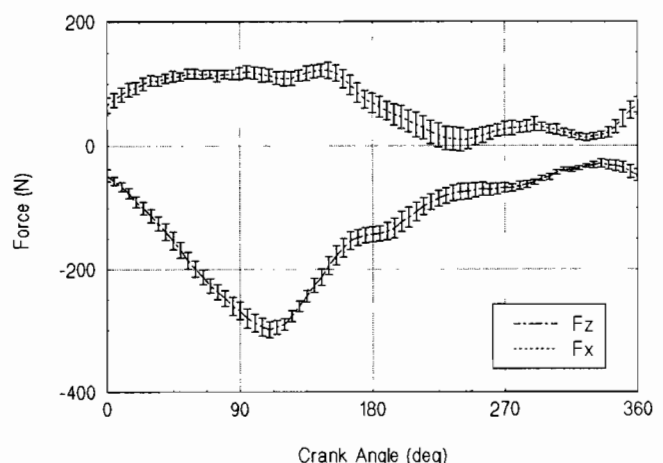


Fig. 5 Averages and standard deviations of normal  $F_z$  and tangential  $F_x$  pedal forces measured over 14 crank cycles at 90 rpm and 250 W: The 0 deg reference is from top dead center and positive is in the direction of rotation

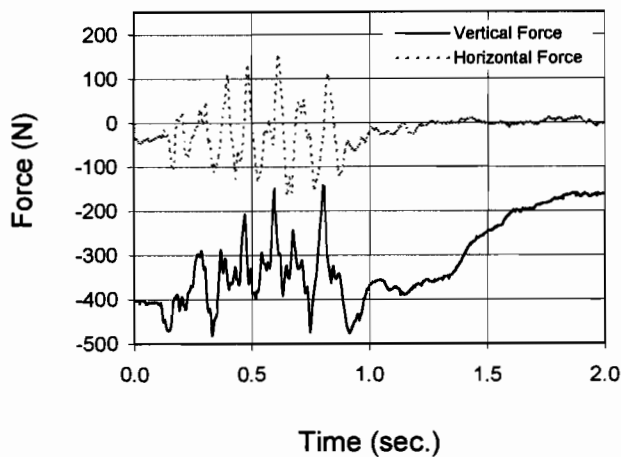


Fig. 6 Sample vertical and horizontal pedal forces measured while coasting at 6.25 m/s over a bumpy track. The subject weighed approximately 800 N and was standing.

dynamic performance capabilities of the dynamometer. The natural frequency of the unloaded pedal was found to be 230 Hz. The natural frequency with a 75 kg person clipped onto the pedal and standing with half of their weight supported was about 137 Hz.

#### Sample Loading Data

To demonstrate the ability of the dynamometer to provide useful information, foot-pedal loads were measured for two cycling situations. One situation measured the loads during steady pedaling at 90 rpm and an average power output from both legs over a full crank cycle of 250 W. The other situation measured dynamic, inertial loads developed as an 800 N subject coasted over a set of bumps with a velocity of 6.25 m/s while standing. The bumps were developed by randomly spacing 2.54-cm-dia wooden dowels perpendicular to the direction of travel along a track approximately 2.5 m in length.

For both cycling situations, the data were recorded by a battery-powered data acquisition computer (Newmiller and Hull, 1990), which the subject carried in a fanny pack. The computer recorded both dynamometer signals, the potentiometer signal indicating the pedal-to-crank angle and an additional potentiometer signal indicating the crank angle at a sampling rate of 200 Hz. The signals from the pedal transducers were routed to the computer along cables strapped to the subject's leg. The flexibility of the cables allowed the subject to move without hindrance. Following collection, the data were uploaded to a personal computer for analysis and display.

For the experienced subject who provided the steady pedaling data, the patterns of loads were highly reproducible, as evidenced by the small standard deviations (Fig. 5). The normal force remained compressive throughout the crank cycle with the peak occurring just after the horizontal crank position as the pedal was moving down. In contrast, the tangential force  $F_x$  remained positive throughout the crank cycle, indicating that the foot was pushing forward on the pedal. These patterns are consistent with those previously reported using a different dynamometer at a comparable pedaling rate and workrate (e.g., Boyd et al., 1996).

While the subject coasted over the bumps in the standing position, the vertical force remained compressive (negative) throughout the trial. The principal effect of the inertial loads was to cause large oscillation in the vertical pedal force from the static value of approximately -400 N (Fig. 6), which developed as a consequence of the subject's position. Note

that the magnitude of this static load is about half the subject's weight, which indicates that little weight was supported by the hands in the standing position. The horizontal pedal force exhibited both positive and negative excursions with the extreme values being approximately equal in magnitude (Fig. 6). These characteristics are similar to those described by Wang (1995), who used a different two-force component dynamometer to measure pedal loads for the same cycling situation as that described here.

#### Discussion

The goal of the work reported in this paper was to design a dynamometric pedal that would provide realistic and accurate measurements of the in-plane force components during off-road cycling. To assess the success of the design presented in reaching this goal, it is useful to evaluate the design critically against the criteria.

One criterion was that the dynamometer accurately measure the two in-plane force components. The design presented meets this criterion for static loads. For the measured  $F_x$  and  $F_z$  force components, the direct sensitivities are very linear and consistent, while the cross sensitivities are calibratable and hence accounted for in the data reduction. For the unmeasured load components, the error introduced by the non-calibratable cross sensitivities is minimal and has little effect on the measurement accuracy of the desired forces.

Owing to the 30 Hz bandwidth that has been reported for pedal loads measured while riding in the standing position over simulated off-road terrain (Wilczynski and Hull, 1994), accurate measurement of dynamic loads was also a criterion. To evaluate both the best-case and worst-case scenarios, the natural frequency was measured in both the unweighted and weighted states. Because the natural frequency of 137 Hz measured in the weighted state exceeds the upper frequency limit (i.e., 30 Hz) by more than 4.5 times, the dynamometric pedal has a sufficient flat response region to measure dynamic loads within 5 percent accuracy (Doebelin, 1990).

To withstand the loads developed both by foot-pedal and ground-pedal interactions, another criterion was that the dynamometric pedal be structurally equivalent to a commercially available design. This criterion was satisfied in part by integrating the dynamometer into a Shimano M737 pedal housing. Thus, the housing is structurally equivalent. To gain sensitivity, however, the spindle, which serves as the sensing element, was reduced in diameter by 2.9 mm. With the use of a material with twice the strength of the original, this reduction leads to a loading capacity nearly equivalent to the M737 pedal spindle. In light of the pedal loading measurements by Wilczynski and Hull (1994), which revealed highest normal forces of about 900 N, the loading capacity for static failure is more than twice this force level. Fatigue strength is not an issue because of the limited use.

The final design criterion was that the dynamometric pedal be functionally equivalent to a Shimano M737 pedal. Since the design uses the M737 housing with no modification to the clipless mechanism, the dynamometer may be used with any SPD-compatible shoe. The only limitation arises due to the desire to keep the instrumentation behind the pedal, and therefore limits use to only one side of the pedal.

The dynamometric pedal differs from the M737 pedal in the manner in which it is fixed to the crank. To simplify the instrumentation, the pedal spindle was fixed to the pedal body and the spindle bearings were relocated to the crank arm. A crank with sufficient material to accommodate the bearings had to be specially selected. Owing to conflicting requirements between bearing load capacity and amount of material available, the bearings used were smaller than desired. Consequently, accelerated wear is anticipated. Considering that the pedal is a research tool, accelerated wear should not limit its utility. Fur-

thermore, when severe wear becomes evident, the bearings may be easily replaced.

### Conclusion

This paper has presented an instrumented pedal suitable for off-road use, which accurately indicates the tangential and normal ( $F_x$  and  $F_z$ ) pedal forces independent of the undesired ( $M_x$ ,  $M_y$ ,  $M_z$ , and  $F_y$ ) loads. The pedal is identical in function to a Shimano M737 pedal, so it does not alter the loading conditions in any way.

As demonstrated by the sample data, this design quantified the pedal forces involved during either pedaling or coasting over off-road bicycling terrain. No other design reported to date has enabled the quantification of pedal loads during off-road cycling. Such a quantification is useful to a variety of purposes ranging from pedaling mechanics to structural design of off-road bicycle components.

### Acknowledgments

The authors would like to thank Shimano for their continuing support and for supplying the M737 pedals used in this project.

### References

- Boyd, T., Hull, M. L., and Wooten, D., 1996, "An Improved Accuracy Six Load Component Pedal Dynamometer for Cycling," *Journal of Biomechanics*, Vol. 29, No. 8, pp. 1105-1110.
- Doebelin, E. O., 1990, *Measurement Systems: Application and Design*, 4th ed., McGraw-Hill, San Francisco, Chap. 3, Section 3.3.
- Hull, M. L., and Davis, R. R., 1981, "Measurement of Pedal Loading in Bicycling," *J. Biomechanics*, Vol. 14, No. 12, pp. 843-872.
- Newmiller, J., Hull, M. L., and Zajac, F. E., 1988, "A Mechanically Decoupled Two Force Component Bicycle Pedal Dynamometer," *J. Biomechanics*, Vol. 21, No. 5, pp. 375-386.
- Newmiller, J., and Hull, M. L., 1990, "A Compact Portable Data Acquisition System for Sports Biomechanics Research," *International Journal of Sports Biomechanics*, Vol. 6, No. 5, pp. 404-414.
- Soden, P. D., and Adeyefa, B. A., 1979, "Forces Applied to a Bicycle During Normal Cycling," *J. Biomechanics*, Vol. 12, No. 7, pp. 527-541.
- Stone, C., 1990, "Rider/Bicycle Interaction Loads During Seated and Standing Treadmill Cycling," Master's Thesis, Department of Mechanical Engineering, UC Davis, CA.
- Vifolias, J., and Alvarez, G., 1992, "Análisis del Comportamiento Ciclista a Traves de Bicicletas Dinamicas Sensorizadas. Simulación Dinamica con Computador," *Jornadas Internacionales Sobre Biomecanica del Ciclismo*, Documento No. 3.
- Wang, E., 1995, "Quantification and Optimization of Off-Road Bicycle Suspension Performance," Ph.D. Dissertation, Department of Mechanical and Aeronautical Engineering, University of California, Davis, CA.
- Wilczynski, H., and Hull, M. L., 1994, "A Dynamic System Model for Estimating Surface-Induced Frame Loads During Off-Road Cycling," *J. Mechanical Design*, Vol. 116, No. 3, pp. 816-822.